Mutational Analysis of Ocriplasmin to Reduce Proteolytic and Autolytic Activity in Pichia Pastoris

Roghayyeh Baghban
Tabriz University of Medical Sciences
Safar Farajnia (farajnias@tbzmedd.ac.ir)
Biotechnology Research center, tabrizUniversity of medical Sciences
Younes Ghasemi
Shiraz University of Medical Sciences
Reyhaneh Hoseinpoor
Shaheed Beheshti University of Medical Sciences
Azam Safary
Tabriz University of Medical Sciences
Mojtaba Mortazavi
Graduate University of Advanced Technology
Nosratollah Zarghami
Tabriz University of Medical Sciences

Research

Keywords: Ocriplasmin, Pichia pastoris, Site-directed mutagenesis, Proteolytic activity, Autolytic activity

Posted Date: August 25th, 2020

DOI: https://doi.org/10.21203/rs.3.rs-62284/v1

Version of Record: A version of this preprint was published on December 13th, 2020. See the published version at https://doi.org/10.1186/s12575-020-00138-0.

Abstract

Background: Ocriplasmin (Jetrea) is using for the treatment of symptomatic vitreomacular adhesion. This enzyme undergoes rapid inactivation and limited activities duration as a result of its autolytic and proteolytic nature after injection within the eye. Moreover, the proteolytic activities can cause photoreceptor damage, which may result in visual impairment in the more serious cases.

Results: The present research aimed to reduce the disadvantages of ocriplasmin using site-directed mutagenesis. To reduce the autolytic activity of ocriplasmin in the first variant, lysine 156 changed to glutamic acid and in the second variant for the proteolytic activity reduction, alanine 59 mutated to threonine. The third variant contained both the mutations. Expression of wild type and three mutant variants of ocriplasmin constructs were done in *Pichia pastoris* expression system. The mutant variants analyzed *in silico* and *in vitro* and compared to the wild type. The kinetic parameters of ocriplasmin variants showed both variants with K156E substitution were more resistant to autolytic degradation than wild-type. These variants also exhibited reduced K_{cat} and V_{max} values. An increase in their Km values, leading to a decreased catalytic efficiency (the K_{cat}/K_m ratio) of autolytic and mix variants. Moreover, in variant with A59T mutation, K_{cat} and V_{max} values have reduced compared to wild type. The mix variants showed the most increase in Km value (almost 2-fold) as well as reduced enzymatic affinity to the substrate. Thus, the results indicated combine mutations at ocriplasmin sequence were more effective compared with single mutations.

Conclusions: The results indicated such variants represent valuable tools for the investigation of therapeutic strategies aiming at non-surgical resolution of vitreomacular adhesion.

Background

Symptomatic vitreomacular adhesion or vitreomacular traction may cause edema, macular distortion and form macular holes. This sight-threatening condition relates to decreased visual acuity, photopsia and metamorphopsia [1–5]. Vitreomacular traction spontaneously clears up in 10–35% of the cases [4, 6, 7]; otherwise, it can progress into visual impairment [1, 8].

Vigilant monitoring and pars plana vitrectomy constitute standard procedures for managing symptomatic vitreomacular adhesion [1, 3]. Given the risk of damage to the optic disc or retina [9, 10] caused by the surgery, proteolytic enzymes such as plasmin have been examined for the enzymatic release of retinal traction [11–13].

Vitreomacular adhesion can be treated and full-thickness macular holes be closed as a result of the activities of the recombinant protease ocriplasmin against the components of the extracellular matrix that form part of the vitreoretinal interface [3, 4, 14, 15]. Two pivotal Phase III trials, including ocriplasmin for Intravitreous Injection-Traction Release without Surgical Treatment [MIVI-TRUST], confirmed the efficacy and safety of ocriplasmin in treating symptomatic vitreomacular adhesion. The Food and Drug Administration therefore approved ocriplasmin in 2012 for treating vitreomacular traction [4, 16]. Active

ocriplasmin comprises 2 polypeptides of 230 and 19 residues, which are connected to each other by 2 disulfide bonds. Four intra-chain disulfide bonds stabilize the domain of 230-residue [17]. Despite obviating the risks associated with the surgery, pharmacologic vitreolysis with ocriplasmin cannot be considered free of any risks [10].

The autolytic and proteolytic nature of this enzyme at physiologic pH limits its duration of activities. Proteolytic activities can cause photoreceptor damage, which may result in visual impairment in more serious cases [18–20]. Moreover, the autolytic degradation of ocriplasmin causes its fast inactivation after vitreous injection [21, 22].

As a highly-promising biocatalyst engineering method, protein engineering can be used to promote enzyme stability and efficiency [23]. Rapid advancements in biological sciences have led up to state-of-the-art protein engineering methods, especially recombinant DNA technology. The random types of these approaches include random mutagenesis and evolutionary techniques such as DNA shuffling. The rational methods include site-directed mutagenesis [24] as an effective yet simple method that introduces special amino acids into target genes using 2 oligonucleotide primers with the desired mutations that complement the opposite strands of a double stranded DNA template [25, 26].

The autolytic cleavage of ocriplasmin is limited to 3 positions, i.e. R177-V178, K166-V167 and K156-E157 as the most important autolytic cleavage site that greatly increases the sensitivity of the other two sites [27]. In addition, the functional activity of plasminogen was found to decrease in dysplasminogenemia. Mutation of Ala601Thr was also described in dysplasminogenemia. The substitution of alanine 601 for threonine was found to play a key role in reducing the activity (alanine 601 in plasminogen is equivalent to alanine 59 in ocriplasmin) [28, 29].

This study designed and generated three mutant variants of ocriplasmin for reducing autolytic and proteolytic activity after *in silico* analysis through introducing single-point mutations. Two variants contained one mutation; to reduce autolytic activities in the first variant (called autolytic variant), lysine 156 mutated to glutamic acid and to reduce proteolytic activities in the second variant (called proteolytic variant), alanine 59 changed to threonine. As the mixed variant, the third one included both the mutations, i.e. A59T and K156E, while the wild type lacked any mutations. All the variants were cloned and expressed in the *Pichia pastoris* expression system. Significant resistance to autolytic inactivation and proteolytic activity was reported in ocriplasmin variants using different assessment methods.

Results

In Silico Analysis of Ocriplasmin Variants

Structural analyses performed using the PIC web server revealed that the substitution of alanine 59 for threonine (A59T (significantly reduces proteolytic activities and the substitution of lysine156 for glutamic acid (K156E) notably affects the autolytic function of the enzyme.

The docking results showed the lower binding affinity of the mutant variants than that of wild-type ocriplasmin. The mutant variants were found able to bind to substrates with high to low affinity. The molecular docking simulations of the substrate S-2403 with different variants of ocriplasmin showed that the minimum free binding energy (DG) between them in the high number conformations cluster were respectively -7.67, -6.93, -6.75, -5.84 kcal/mol for substrate-wild type ocriplasmin, substrate-autolytic type ocriplasmin, substrate-proteolytic type ocriplasmin and substrate-mixed type ocriplasmin. Fig. 1 (a-d) shows two-dimensional amino acids which interacted and made hydrogen bonds with ocriplasmin variants. The images were prepared using Lig Plot v1.4.4 software.

Computational simulations using RMSD, RMSF and center of mass average distances showed more affinity of the substrate S-2403 to the wild-type than mutant variants. The average RMSD was respectively obtained as 0.33, 0.34 and 0.39 nm for the three mutant variants of ocriplasmin in the complex with the substrate-proteolytic, substrate-autolytic, and substrate-mixed type and an average RMSD of 0.28 nm was derived for the substrate-wild type ocriplasmin throughout the simulation.

The RMSF values of the active site located residues, i.e. His61, Asp104 and Ser199, in the mutant structure of ocriplasmin-substrate complex were greater than that of the wild type. These values were relatively stable in the wild protein structure compared to in the mutant types, mainly owing to more interactions between the substrate and wild-type ocriplasmin. The results are shown in Fig. 2 (a-c).

Construction of Ocriplasmin Variants

Table 1 presents the sequences of primers used for this recombination. The synthesized ocriplasmin gene and the three mutant ocriplasmin variants were cloned in the pPinkα-Hc plasmid downstream from the AOX1 promoter after being generated through site-directed mutagenesis. Then the linearized pPinkα-Hc-ocriplasmin vectors were introduced into *P. pastoris* cells and positive clones were confirmed using PCR (Fig. 3).

Expression and Optimization of Ocriplasmin Variants in *P. pastoris*

Recombinant plasmid with the wild-type and plasmids-containing mutated versions of the gene were transformed into *P. pastoris* cells. The relative expression level of a protein was shown by the color of the colonies. Small and high amounts of ADE2 gene products were respectively shown by pink and white colonies, whereas the latter contained a higher number of copies of an integrated construct. The secretory expression of all variants was performed in the BMMY medium. Then, the effect of different factors was evaluated to obtain optimal culture conditions for the ocriplasmin expression yield. The highest yield of ocriplasmin, i.e. approximately 0.2 mg/ml with a 93.6 % purity, was achieved at pH=6, a temperature of 30 °C, a methanol concentration of 0.5-1 %, a duration of 72 hours and a medium comprising 1 % yeast extract, 2 % peptone and 1 % tryptone. The secretory expression and optimization of all the variants was analyzed and a 27 kDa protein band detected through SDS-PAGE related to the molecular weight of ocriplasmin as per Fig. 4a.

Characterization of Ocriplasmin Variants

Immunoblotting confirmed this finding, and the complete protein was recognized in a denatured form with a single band of approximately 27 kDa using the anti-plasminogen polyclonal antibody as per Fig. 4b.

Specificity Determination

According to Fig. 4c, the specificity of ocriplasmin toward the antibody was determined using ELISA, which was performed with the anti-plasminogen antibody raised in rabbit and confirmed the functionality of the *P. pastoris* expressed recombinant ocriplasmin.

Activation of Ocriplasmin Variants and Autolytic/proteolytic Activity Measurement

The inactive zymogen forms of ocriplasmin variants generated in *P. pastoris* were transformed into catalytically-active forms by the use of urokinase after purification. The activity of the aliquots collected at different times as well as the amount and rate of conversion into the active forms were monitored. This activity was maximized within 30 min in the empirical conditions applied. The conversion of the zymogen and the activity were maximized simultaneously. According to Fig. 5, SDS–PAGE was conducted to confirm the activation process.

HydrolyticActivity Assay

Fixed concentrations of enzyme variants were exposed to different concentrations of substrate for 0-20 minutes to form a colored (yellow) product. It has shown that the color intensity (product formation) in mutant variants has much rapid reduction than wild-type. Reduced activity of mutant variants was also confirmed by reducing the optical density at 405 nm (Fig. 6). The results showed that A59T and K156E mutations have a significant effect on the hydrolytic activity of mutant variants compared to the wild type. These mutations reduced the enzyme catalyze ability.

Kinetic Evaluations

According to Fig. 7(a-d) and the results presented in Table 2, the kinetic parameters of the wild-type and mutant variants of ocriplasmin with the substrate S-2403 were calculated on the basis of the Michaelis–Menten plot at 37 °C. K_m was obtained as 908.4 μM for wild variant of ocriplasmin, 906.7 μM for the proteolytic-type, 989.8 μM for the autolytic and 1704 μM for the mixed variant. Given that the lowest K_m was associated with the proteolytic-type, this variant had a higher affinity to S-2403 compared to other variants. V_{max} of the wild-type (0.123 μmol/mg/min) was the highest compared to 0.0784, 0.092 and 0.1081 of the mutant variants. The hydrolytic efficiency of the wild-type ocriplasmin was therefore higher than that of the mutant variants.

The values of the kinetic parameters obtained from the proposed model provided valuable knowledge on the enzyme nature. The rate of a reaction is halved compared to the maximum rate at a substrate

concentration of K_m. This constant also negatively relates to the substrate affinity to the enzyme. In other words, the higher the K_m, the lower the affinity. As a result, the rate will be maximized at a lower substrate than at a lower K_m. In addition, K_{cat} reflects the speed of a reactions, whereas K_{cat}/K_m shows the efficiency of an enzyme in converting a substrate to a product. A nonlinear regression model can be employed to explain the relationship of the substrate concentration and the reaction speed based on Michaelis-Menten kinetics.

Discussion

Ocriplasmin is non-surgical alternative for the treatment of symptomatic vitreomacular traction. Its proteolytic activity at physiologic pH and natural vulnerability to autolytic inactivation can influence its efficacy *in vivo* and lead to serious damages [17].

In the present study, a series of site-directed mutagenesis performed in cDNA encoding ocriplasmin to reduce its autolytic and proteolytic activity, using two overlapping primers containing the desired mutations. Site-directed mutagenesis is a powerful tool to create specified pools of protein variants [30]. This technique has been effectively used in many studies to improve proteins and enzymes properties, such as; improved stability and specificity [31], generate mutants with increased thermostability, efficiency and half-lives compare to the wild-type enzyme [32] and improved activity towards substrate [13].

Among three autolytic cleavage sites in ocriplasmin (K156–E157, K166–V167 and R177–V178), lysine 156 was chosen to change to glutamic acid in order to reduce autolytic activity [27]. Previous studies revealed that initial cleavage occurs at position 156–157 because it is faster and after this cleavage, sensitivity of the other two sites to autolytic cleavage greatly enhances [27]. Cleavage at 156–157 site was caused inactivation, and mutant with cleavage at 177–178 site was detected in wild-types [17]. Therefore, K156E substitution is more effective on autolytic function rather than other two.

Clinical data from Aoki et al. was used to design a variant to reduce proteolytic activity of ocriplasmin. They investigated a patient with chronic thrombosis and the only abnormality was low plasminogen in plasma [33]. According to Miyata et al. the abnormality in plasminogen is because of Ala601Thr replacement in codon 601 of exon XV owing to the G to A nucleotide transition [34]. Val355Phe and Asp676Asn point mutations in the plasminogen gene also have been found in patients with dysPLGemia [35]. Given that ocriplasmin is the truncated version of human plasmin, and alanine 601 in plasmin is equal to alanine 59 in ocriplasmin, we hypothesized that substitution of alanine 59 with other amino acid (here, threonine) possibly will has an effect on reducing the proteolytic activity of the enzyme.

Three ocriplasmin variants with A59T, K156E and A59T and K156E mutations simultaneously, were designed. Mutational analysis of ocriplasmin variants was performed by homology modeling, molecular dynamics simulations, and molecular docking studies. *In silico* mutational analysis of ocriplasmin revealed that A59T and K156E substitution have significant effect on the reduction of proteolytic and

autolytic activity, respectively. As expected, reduced autolytic and proteolytic function was confirmed using docking study and MD simulation as diminished binding affinity of mutant variants to the substrate rather than wild type.

After *in silico* analyses of designed mutant variants, wild-type and three mutant ocriplasmin (proteolytic, autolytic and mixed variants) was constructed using site-directed mutagenesis and their expression in *P. pastoris* was studied and confirmed by western blot. A59T and K156E mutations reduced hydrolytic activity and the enzyme catalytic function. The product formation of mutant variants presented much rapid reduction, compared to the wild-type.

The kinetic parameters of wild type and mutant variants of ocriplasmin showed both variants with K156E substitution (autolytic and mixed variants) were more resistant to autolytic degradation than wild-type. These variants exhibited an increase in their Km values, leading to a decreased catalytic efficiency (the K_{cat}/K_m ratio). The autolytic and mixed variants also exhibited reduced K_{cat} and V_{max} values. This results were in agreement with Noppen et al.[17]. Also, reduced K_{cat} and V_{max} values was observed in variant with A59T mutation. The variants with both mutations showed the most increase in Km value (almost 2-fold) as well as reduced enzymatic affinity to the substrate. Thus, the results indicated combine mutations at ocriplasmin sequence were more effective compared with single mutations.

Conclusions

Mutational analysis of ocriplasmin enzyme revealed that A59T and K156E mutagenesis could be used for the development of new ocriplasmin variants with better autolytic and proteolytic activity, as a result higher therapeutic efficacy.

Materials & Methods

In Silico Methods for Mutational Analysis of Ocriplasmin Variants

The undesirable autolytic and proteolytic activities of ocriplasmin can be reduced with site-directed mutagenesis leading to an enzyme with improved catalytic activities and half-life. Three ocriplasmin variants were designed for improving biological/physicochemical characteristics. The structural analyses of all the variants, i.e. the wild type and the three mutants, were performed using a protein interaction calculator (PIC) server available at crick.mbu.iisc.ernet.in/PIC. A molecular docking simulation was performed using the freely available package Auto Dock 4.2.6 and Auto Dock Tools 1.5.6 software to study interactions between substrate S-2403 and ocriplasmin variants, and binding capability was evaluated by calculating the free binding energy. The conformational features of protein-substrate complexes for all the variants was evaluated in a 100-ns Molecular Dynamics Simulation using the GROMACS 2016 package.

Construction and Cloning of the Ocriplasmin Expression Vector

The ocriplasmin coding sequence (DB08888 (DB05028)) was optimized and synthesized (GenScript) for the best expression in *P. pastoris*. The primers used to amplify the ocriplasmin gene included 5'-CTATTGCCAGATTGCTGC-3' and 5'-GCGTGAATGTAAGCGTGAC-3'. Moreover, *Kpn*I and *Xho*I (TaKaRa Biotech) were used to digest the purified PCR product, and then ligated into pPinkα-HC (Thermo Fisher Scientific) under the control of the alcohol oxidase I (AOX1) promoter. Afterwards, pPinkα-HC-ocriplasmin as the new construct was transformed to the *E. coli* DH5-alpha (Thermo Fisher Scientific). To select the clones, the transformants were plated onto Luria-Bertani (LB) agar containing 100 mg/ml of ampicillin (Sigma-Aldrich). The recombinant constructs extracted from the ampicillin-resistant clones were confirmed with colony PCR and restriction digestion.

Mutant Construction Using Site-directed Mutagenesis

The optimized coding sequence of the ocriplasmin gene was employed as a template for the amplification.

Glutamic acid was substituted for lysine 156 (K156E) in SOEing PCR to construct the mutant variant and reduce *autolytic* activities. Amplification was first performed on a 481 bp DNA fragment, containing the 5' end of the ocriplasmin gene and upstream sequences (with α factor-F1 and OCR-R2 primers), and a 330 bp fragment, including the 3' end of the gene and downstream sequences (with OCR-F2 and CAC1-R1 primers). To generate mutated fragments containing the desired point mutations, in the second round, amplified fragments were joined using the splicing by overlap extension PCR method [36].

Alanine 59 changed to threonine (A59T) to construct the mutant fragment and reduce proteolytic activities. Amplification was performed on a 190 bp DNA fragment, including the 5' end of the ocriplasmin gene and upstream sequences (with α factor-F1 and OCR-R3 primers) and a 617 bp fragment, including the 3' end of the ocriplasmin gene and downstream sequences (with OCR-F3 and CAC1-R1 primers). Splicing by overlap extension was performed in the second round of PCR to join these fragments together [36] and generate a PCR fragment including the desired point mutations.

To produce the mutant fragment containing both the mutations, A59T and K156E, the fragment with A59T mutation was used as a template for adding K156E change as per the same steps described.

These mutated PCR fragments were cloned into *Xho*I and *Kpn*I restriction sites of the pPinkα-HC vector and transferred into the *E. coli* DH5-alpha. PCR and plasmid digestion confirmed the cloning and sequencing confirmed the mutations.

Transformation and Selection in *P. pastoris*

The recombinant pPinkα-HC-ocriplasmin vectors extracted and linearized with *Spe*I. *P. pastoris* strain 4 competent cells (Thermo Fisher Scientific) were prepared and transformed with 5-10 µg linearized plasmids by electroporation for the wild type and three mutant variants of ocriplasmin. The transformations were recovered at 30 °C in yeast extract peptone dextrose with sorbitol (YPDS) for 2-12 hours. The cell mixture spread on minimal dextrose (MD) plates was incubated at 30 °C for 3-10 days to

obtain distinct colonies. Colony PCR was performed using specific primers to confirm the clones that integrated heterologous expression cassettes.

Small Scale Expression and Optimization in *P. pastoris*

For the small-scale expression, the wild-type and mutant colonies inoculated from the fresh transformation plates in 10 ml buffered glycerol complex (BMGY) medium were incubated in a shaking incubator for 1-2 days at 24-30 °C until an optical density (OD600) of 4-6 was obtained. After transferring the cells into 50-ml of fresh BMGY medium, they were incubated for one day until obtaining an OD600 of 5-6. To induce the ocriplasmin expression, the cells were transferred to buffered methanol complex (BMMY) medium. The induced cultures underwent a four-day incubation at 150 rpm and 30 °C and were fed, every 24 hours, with methanol at a final concentration of 0.5 %. The supernatant was collected at 24, 48, 72 and 96 hours for analyzing the protein expression.

The culture conditions under which the ocriplasmin expression was optimized in the adenine-deficient *P. pastoris* strain included cell density=one and two fold, pH=3-7, temperature=20, 25 and 30 °C, concentrations of glycerol=5-10 %, methanol=0.25-8 % and ammonium sulfate=5-20 % and induction time=1-4 days. Sodium dodecyl sulfate-polyacrylamide gel electrophoresis (SDS-PAGE) and immunoblotting were performed to analyze the samples of the supernatants.

Production of Anti-Plasminogen Polyclonal Antibody in Rabbit

Anti-plasmin antibodies can help detect ocriplasmin as a truncated version of recombinant human plasmin. A male New Zealand white rabbit was immunized with four intradermal injections on days 1, 14, 23 and 31. The first and the following three injections comprised a mixture of 150 µg of plasminogen protein (Sigma-Aldrich) in 0.3 ml of saline respectively emulsified in 0.3 ml of Freund's Complete Adjuvant and Freund's Incomplete Adjuvant. The blood samples collected from the ears of the rabbit before every immunization and kept for two hours at 4 °C for coagulation. The serum separated from the coagulated blood was kept at -20 °C. Western blotting and enzyme-linked immunosorbent assay (ELISA) were performed to quantitatively and qualitatively evaluate the produced antibody.

Specificity Determination

The specificity of interactions between ocriplasmin expressed in *P. pastoris* and anti-plasminogen antibody produced in rabbits was determined using ELISA. The wells were coated overnight with 10 µg/ml of recombinant ocriplasmin in carbonate-bicarbonate buffer with pH 7.2 at 4 °C. The plates were rinsed three times using phosphate-buffered salin (PBS) with 0.05 % Tween 20. 100 µl of different dilutions (1/400, 1/800, 1/1600, 1/3200, 1/6400, 1/12800, 1/25600) of rabbit serum containing the anti-plasminogen antibody was added to the wells. After one-hour incubation, the plates were rinsed and incubated for one hour using 1: 5,000 dilutions of the HRP-conjugated anti-rabbit antibody. The TMB substrate was added after washing, and the reaction was stopped 20 min later using a 1 N H_2SO_4. The absorption was ultimately read at 450 nm.

Immunoblotting

The recombinant ocriplasmin secreted from *P. pastoris* underwent immunoblotting by separating cell lysate proteins through SDS-PAGE and then transferring them to a polyvinylidene difluoride membrane (Thermo Fisher Scientific). A solution of 3 % (w/v) bovine serum albumin in TBS (tris-buffered saline) with 0.1 % Tween 20 blocked the membrane. Ocriplasmin was detected using an anti-plasminogen antibody produced in rabbit and HRP-conjugated goat anti-rabbit IgG as a secondary antibody (Sigma-Aldrich). Enhanced chemiluminescence (ECL) (Thermo Fisher Scientific) was then used to detect proteins.

Activation of Ocriplasmin Variants

A urokinase plasminogen activator (Sigma-Aldrich) was utilized to transform the purified ocriplasminogen variants into the corresponding active forms. Solutions of the ocriplasminogen variants with concentrations of 5-20 mM were incubated at 37 ^{o}C in the presence of the urokinase at a ocriplasminogen to urokinase ratio of 100/2 and 100/5. After completing the phase of activation, SDS-PAGE was performed to evaluate the transformed ocriplasminogen.

Measuring HydrolyticActivities

The hydrolytic activities of active ocriplasmin species extracted were monitored against S-2403™ (Chromogenix) as a substrate explained by Aerts et al. in 2012 [27]. The initial release rate of p-nitroaniline was monitored at 405 nm using Chromogenix S-2403™ to measure the hydrolytic activity of ocriplasmin. 1-10 nM ocriplasmin and 0.3 mM S-2403 substrate was used. Finally, the measured activities of wild type were compared with the hydrolytic activities determined for the mutant variants.

Characterizing the Kinetic Parameters; the Michaelis Constant (K_m), the Catalytic Rate (K_{cat}) and V_{max}

Initial hydrolysis rates were measured at different concentrations of S-2403 as the substrate to obtain the kinetic parameters of ocriplasmin variants. The mutant and wild-type enzymes were aliquoted in a duplicate manner to volumes of 75 µl to obtain a fixed concentration and the substrate was added at concentrations of 2.4, 1.2, 0.6, 0.3, 0.15 and 0.075 mM. After measuring the absorbance at 405 nm every 5 minute, a standard curve was employed to calculate the micromoles of the released product per minute. Linear regression was used to calculate K_{cat}, K_m and V_{max} based on equation (1), in which [S] represents the concentration of S-2403 and [OCR] that of active ocriplasmin. Moreover, K_{cat} and K_m could be calculated by analyzing total hydrolysis curves derived at [S] and V_{max} using equation (2). The data were fitted to the Michaelis–Menten equation using GraphPad Prism software (version 8.0.2). The measurements were performed at 37 ^{o}C and in a mixture of 38 mM NaCl, 50 mM Tris-HCl and 0.01 % Tween 80 with pH=7.4.

$$V_i = \frac{k_{cat}.[\mathrm{OCR}].[S]}{K_m+[S]} \quad (1)$$

$$A_t = \left[(A_0 - A_\infty).e^{-\frac{k_{cat}}{k_m}[\mathrm{OPL}]t}\right] + A_\infty \quad (2)$$

Abbreviations

VMA: vitreomacular adhesion; VMT: vitreomacular traction; PPV: pars plana vitrectomy; SDM: site-directed mutagenesis; PIC: protein interaction calculator; MDS: Molecular Dynamics Simulation; RMSD: root mean square deviation; RMSF: root mean square fluctuation; BMMY: Buffered Methanol-complex Medium; BMGY: Buffered Glycerol Complex Medium; MD plate: Minimal Dextrose plate; YPDS: yeast extract peptone dextrose with sorbitol

Declarations

Acknowledgments

The authors like to thank the Biotechnology Development Council of the Islamic Republic of Iran and also Tabriz University of medical science, Tabriz, Iran, for supporting this study.

Authors' Contributions

SF and RB conceived and designed research. RB conducted experiments. YG contributed to the experimental development. RH edited the manuscript. AS analyzed data. MM analyzed data. All authors read and approved the manuscript.

Funding

This study was funded by Biotechnology Research Center, Tabriz University of Medical Sciences, Tabriz, Iran (grant number 57829).

Availability of Data and Materials

All data and materials are within the paper.

Ethics Approval and Consent to Participate

This article does not contain any studies with human participants or animals performed by any of the authors.

Consent for Publication

All authors have read and approved the final version of the manuscript.

Competing Interests

The authors declare that they have no conflict of interests.

References

1. Amoaku W, Cackett P, Tyagi A, Mahmood U, Nosek J, Mennie G, et al. Redesigning services for the management of vitreomacular traction and macular hole. Eye. 2014;28(1):S1-S10.
2. García-Layana A, García-Arumí J, Ruiz-Moreno JM, Arias-Barquet L, Cabrera-López F, Figueroa MS. A review of current management of vitreomacular traction and macular hole. J Ophthalmol 2015;2015.
3. Mec-Słomska AE, Adamiec-Mroczek J, Kuźmicz E, Misiuk-Hojło M. Intravitreal ocriplasmin: A breakthrough in the treatment of vitreomacular traction? Adv Clin Exp Med. 2017;26(3):527-31.
4. Stalmans P, Benz MS, Gandorfer A, Kampik A, Girach A, Pakola S, et al. Enzymatic vitreolysis with ocriplasmin for vitreomacular traction and macular holes. N Engl J Med. 2012;367(7):606-15.
5. Steel DH, Lotery AJ. Idiopathic vitreomacular traction and macular hole: a comprehensive review of pathophysiology, diagnosis, and treatment. Eye. 2013;27(1):S1-S21.
6. Almeida D, Chin EK, Folk JC, Rahim K, Russell SR. Predictive factors for the spontaneous resolution of vitreomacular traction. Investig Ophthalmol Vis Sci. 2014;55(13):327-.
7. Stalmans P. A retrospective cohort study in patients with tractional diseases of the vitreomacular interface (ReCoVit). Graefes Arch Clin Exp Ophthalmol. 2016;254(4):617-28.
8. Hikichi T, Yoshida A, Trempe CL. Course of vitreomacular traction syndrome. Am J Ophthalmol 1995;119(1):55-61.
9. Vander JF, Kleiner R. A method for induction of posterior vitreous detachment during vitrectomy. Retina (Philadelphia, Pa). 1992;12(2):172-3.
10. Han DP, Abrams GW, Aaberg TM. Surgical excision of the attached posterior hyaloid. Arch Ophthalmol 1988;106(7):998-1000.
11. Sebag J. Pharmacologic vitreolysis. Retina. 1998;18(1):1-3.
12. Trese M. Enzymatic-assisted vitrectomy. Eye. 2002;16(4):365-8.
13. Trese MT, editor Enzymatic vitreous surgery. Seminars in ophthalmology; 2000: Taylor & Francis.
14. Bennison C, Stephens S, Lescrauwaet B, Van Hout B, Jackson TL. Cost-effectiveness of ocriplasmin for the treatment of vitreomacular traction and macular hole. J Mark Access Health Policy. 2016;4(1):31472.
15. Dugel PU, Tolentino M, Feiner L, Kozma P, Leroy A. Results of the 2-year ocriplasmin for treatment for symptomatic vitreomacular adhesion including macular hole (OASIS) randomized trial. Ophthalmology. 2016;123(10):2232-47.

16. Khanani AM, Duker JS, Heier JS, Kaiser PK, Joondeph BC, Kozma P, et al. Ocriplasmin Treatment Leads to Symptomatic Vitreomacular Adhesion/Vitreomacular Traction Resolution in the Real-World Setting: The Phase IV ORBIT Study. Ophthalmol Retina. 2019;3(1):32-41.
17. Noppen B, Fonteyn L, Aerts F, De Vriese A, De Maeyer M, Le Floch F, et al. Autolytic degradation of ocriplasmin: a complex mechanism unraveled by mutational analysis. Protein Eng Des Sel. 2014;27(7):215-23.
18. Ponce CMP, Stevenson W, Gelman R, Agarwal DR, Christoforidis JB. Ocriplasmin: who is the best candidate? Clin Ophthalmol 2016;10:485.
19. Figueroa MS, Contreras I. VA 2. Vitreomaculopathy Surgery. Vitreous: Springer; 2014. p. 571-600.
20. Kamei M, Nishida K. Understanding the Adverse Effects of Ocriplasmin. 2015.
21. Stalmans P, Girach A. Vitreous levels of active ocriplasmin following intravitreal injection: results of an ascending exposure trial. Investig Ophthalmol Vis Sci. 2013;54(10):6620-7.
22. Bandello F, La Spina C, Iuliano L, Fogliato G, Parodi MB. Review and perspectives on pharmacological vitreolysis. Ophthalmologica. 2013;230(4):179-85.
23. Gupta MN. Enzyme function in organic solvents. Eur J Biochem. 1992;203(1-2):25-32.
24. Arnold FH. Engineering proteins for nonnatural environments. FASEB J. 1993;7(9):744-9.
25. Turanli-Yildiz B, Alkim C, Cakar ZP. Protein engineering methods and applications: INTECH Open Access Publisher; 2012.
26. Antikainen NM, Martin SF. Altering protein specificity: techniques and applications. Bioorg Med Chem. 2005;13(8):2701-16.
27. Aerts F, Noppen B, Fonteyn L, Derua R, Waelkens E, de Smet MD, et al. Mechanism of inactivation of ocriplasmin in porcine vitreous. Biophys Chem. 2012;165:30-8.
28. Tefs K, Gueorguieva M, Klammt Jr, Allen CM, Aktas D, Anlar FY, et al. Molecular and clinical spectrum of type I plasminogen deficiency: a series of 50 patients. Blood. 2006;108(9):3021-6.
29. Song KS, Lee SM, Choi JR. Detection of an Ala601Thr mutation of plasminogen gene in 3 out of 36 Korean patients with deep vein thrombosis. J Korean Med Sci. 2003;18(2):167.
30. Mingo J, Erramuzpe A, Luna S, Aurtenetxe O, Amo L, Diez I, et al. One-tube-only standardized site-directed mutagenesis: an alternative approach to generate amino acid substitution collections. PloS one. 2016;11(8).
31. Gupta R, Beg Q, Lorenz P. Bacterial alkaline proteases: molecular approaches and industrial applications. Appl Microbiol Biotechnol. 2002;59(1):15-32.
32. Duan X, Chen J, Wu J. Improving the thermostability and catalytic efficiency of Bacillus deramificans pullulanase by site-directed mutagenesis. Appl Environ Microbiol. 2013;79(13):4072-7.
33. Aoki N, Moroi M, Sakata Y, Yoshida N, Matsuda M. Abnormal plasminogen: a hereditary molecular abnormality found in a patient with recurrent thrombosis. J Clin Invest. 1978;61(5):1186-95.
34. Miyata T, Iwanaga S, Sakata Y, Aoki N. Plasminogen Tochigi: inactive plasmin resulting from replacement of alanine-600 by threonine in the active site. Proc Natl Acad Sci. 1982;79(20):6132-6.

35. Kida M, Masuyo H, Yamazaki T, Ichinose A. Presence of two plasminogen alleles in normal populations. Thromb Haemost. 1998;59(01):150-4.
36. Horton RM, Ho SN, Pullen JK, Hunt HD, Cai Z, Pease LR. [17] Gene Splicing by Overlap Extension. Methods Enzymol 1993;217(C):270-9.

Tables

Table 1 The sequences of the primers used for amplification of Ocriplasmin variants

Variants	5′ sequence 3′
Wild	α factor-F1: CTATTGCCAGATTGCTGC CAC1-R1: GCGTGAATGTAAGCGTGAC
Proteolytic	OCR-F2 : GGTGCTGGTTTGTTGGAAGAAGCTCAATTGC OCR-R2: CAATTGAGCTTCTTCCAACAAACCAGCACCG
Autolytic	OCR-F3 : AGAATGGGTTTTGACTACTGCTCACTGTTTGG OCR-R3: CCAAACAGTGAGCAGTAGTCAAAACCCATTCT
Mixed	OCR-F4 : CGGTGCTGGTTTGTTGGAAGAAGCTCAATTGC OCR-R4 : GCAATTGAGCTTCTTCCAACAAACCAGCACCG

Table 2 kinetic parameters of the wild-type and mutant variants of ocriplasmin with the substrate S-2403

Ocriplasmin variants **Kinetic parameters**	**Wild**	**Proteolytic**	**Autolytic**	**Mixed**
Vmax	0.123	0.0784	0.092	0.1081
Km	908.4	906.7	989.8	1704
Kcat	12.28	7.836	9.217	10.81
Kcat/Km	0.0135	0.0086	0.0093	0.0063

Figures

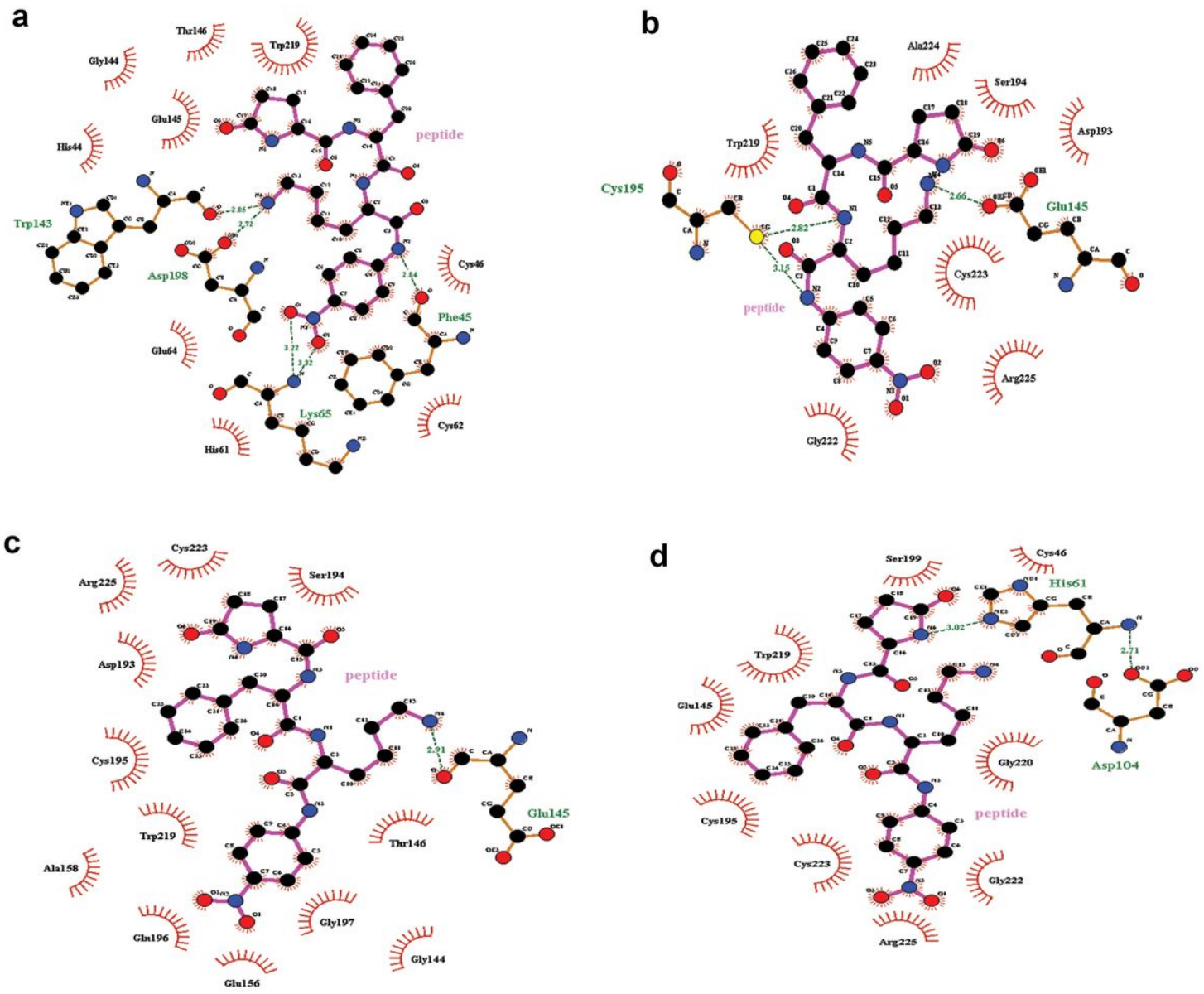

Figure 1

Molecular interactions between S-2403 substrate and amino acids of ocriplasmin presented by 2-D mode. The formed hydrogen bonds among amino acids and substrate presented by green spheres in, a peptide-wild type ocriplasmin, b peptide-proteolytic type ocriplasmin, c peptide-autolytic type ocriplasmin and, d peptide- mixed type ocriplasmin in the docked systems

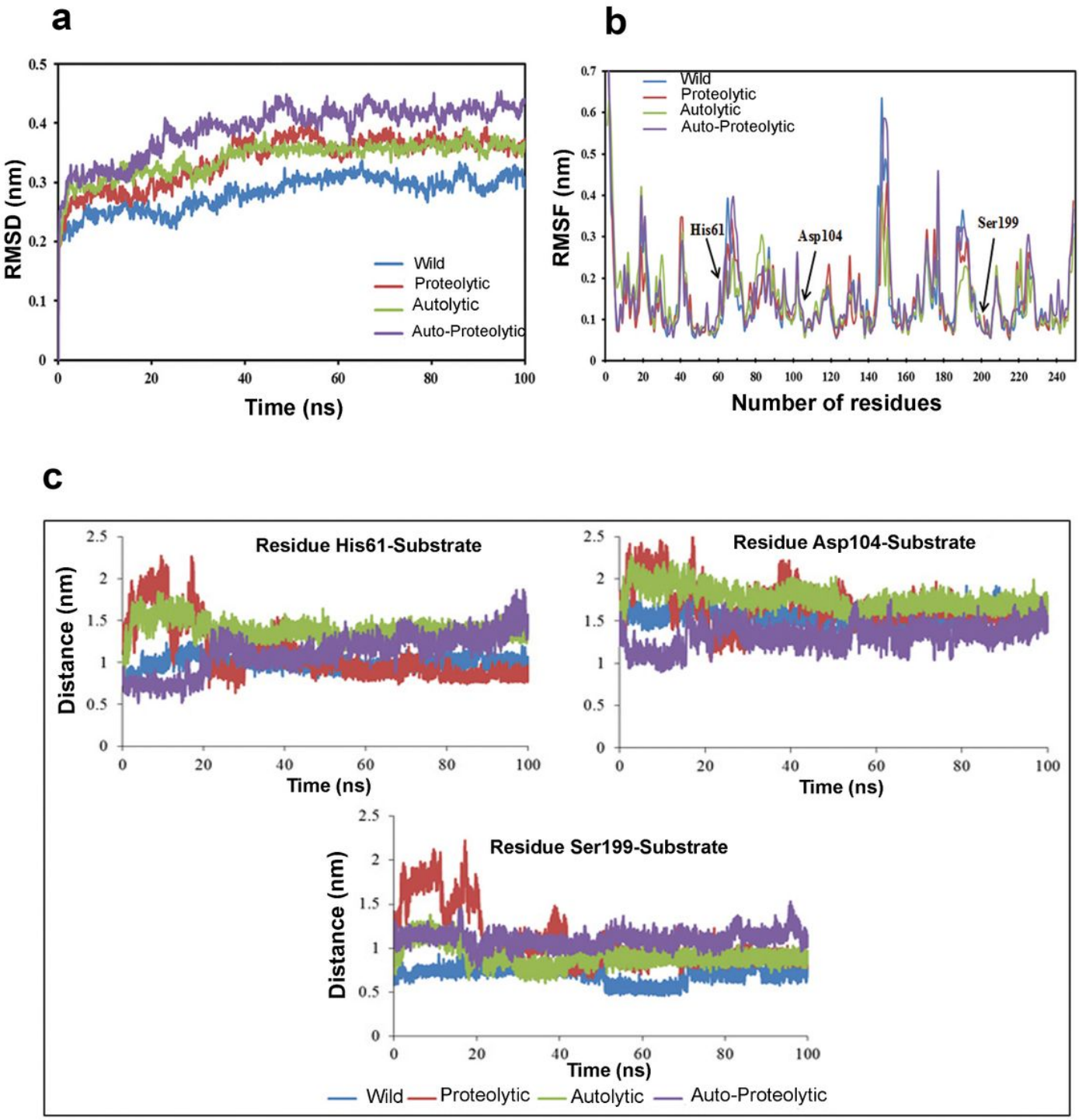

Figure 2

a Backbone RMSD are shown as a function of time for wild type and mutant variants. b RMSF of the backbone CAs of C-alpha atoms of wild type and mutant variants. c Comparison distance between center of mass of ocriplasmin and substrate; It shows the effective vicinity of wild type rather than mutant variants of ocriplasmin. Wild type (blue) and mutant variants, proteolytic (red), autolytic (green) and mixed (dark violet)

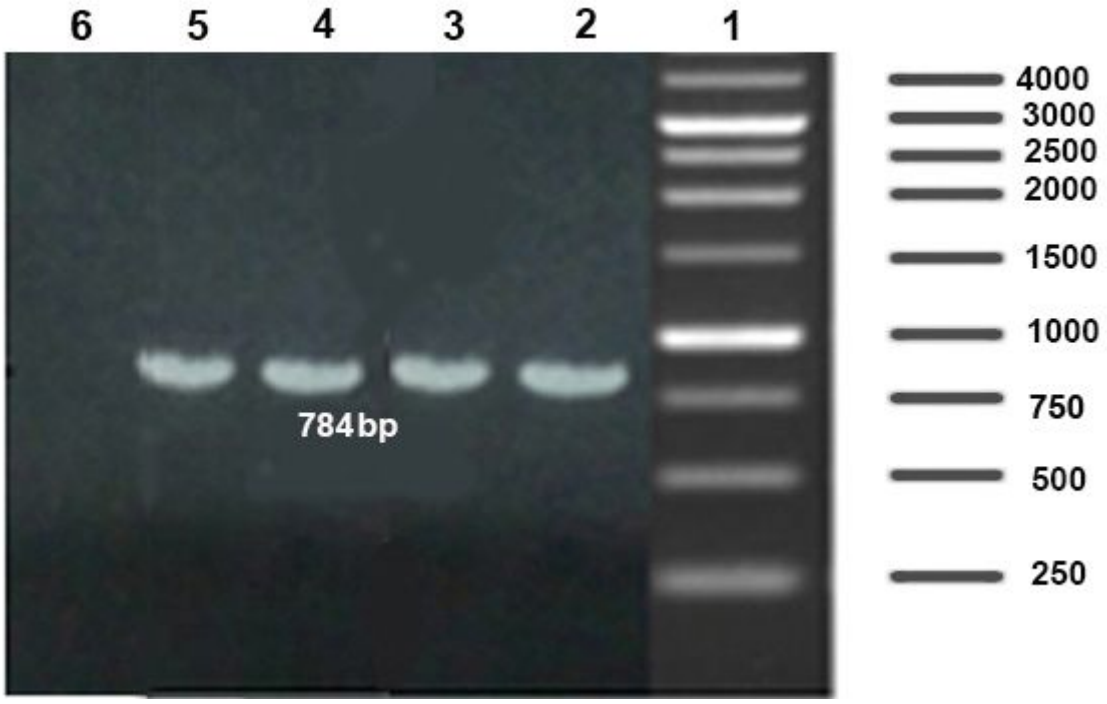

Figure 3

Confirmation of recombinant wild type and mutant clones screened by PCR. Column 1: DNA ladder, Column 2: PCR products (784 bp) of wild type, Column 3-5: PCR products (784 bp) of autolytic, proteolytic and mixed variants, respectively. Column 6: Negative control

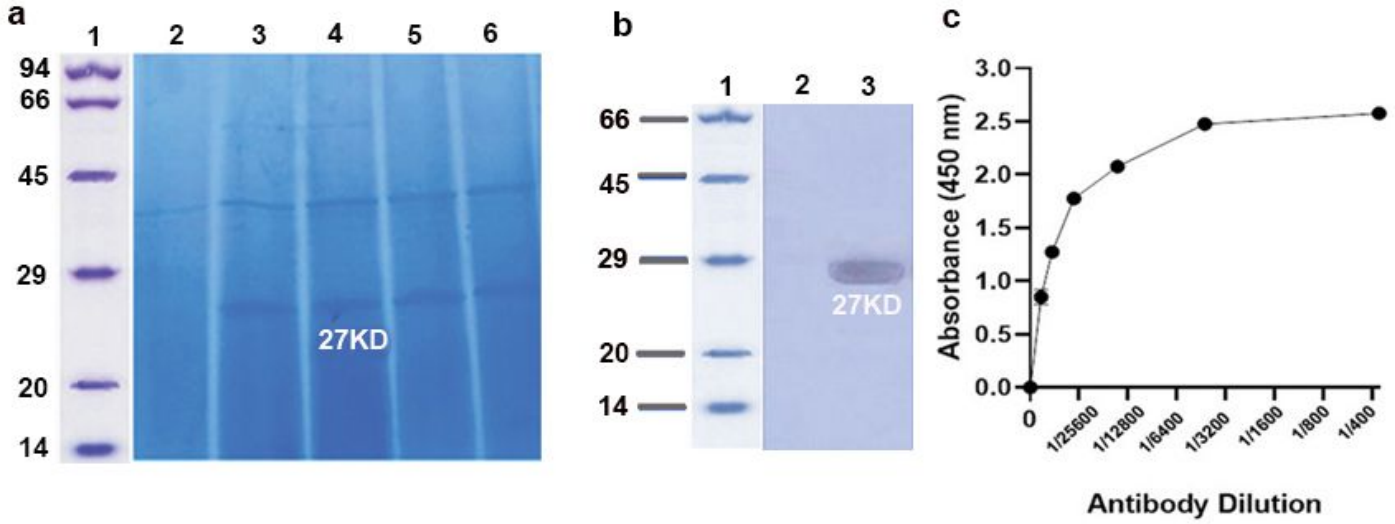

Figure 4

a Expression of ocriplasmin after optimization in Pichia pastoris. Column 1: Protein marker, Column 2: Negative control, (P pastoris none transformed) Column 3-6: a 27 KDa protein product relating wild-type, autolytic, proteolytic and mixed variants, respectively. b Western blotting, Column 1: Protein marker, Column 2: Negative control, Column 3: Purified ocriplasmin (a 27 KDa protein product) expressed in

Pichia pastoris. c Elisa assay using anti-plasminogen antibody and recombinant protein expressed in Pichia pastoris

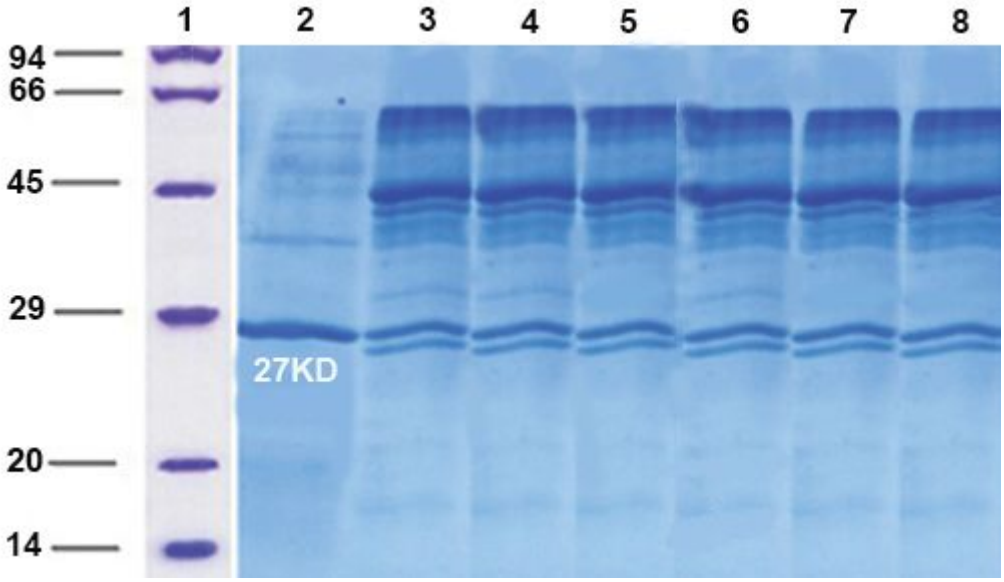

Figure 5

Activation of ocriplasmin by urokinase. Reducing SDS–PAGE illustrating that activation with urokinase is almost complete within 30 min. Ocriplasmin (27 KD) is converted into two fragments upon activation. Column 1: Protein marker, Column 2: Ocriplasmin before activation, Column 3-5: Samples collected 10, 30 and 60 min after addition of 2 % urokinase. Column 6-8: Samples collected 10, 30 and 60 min after addition of 5 % urokinase

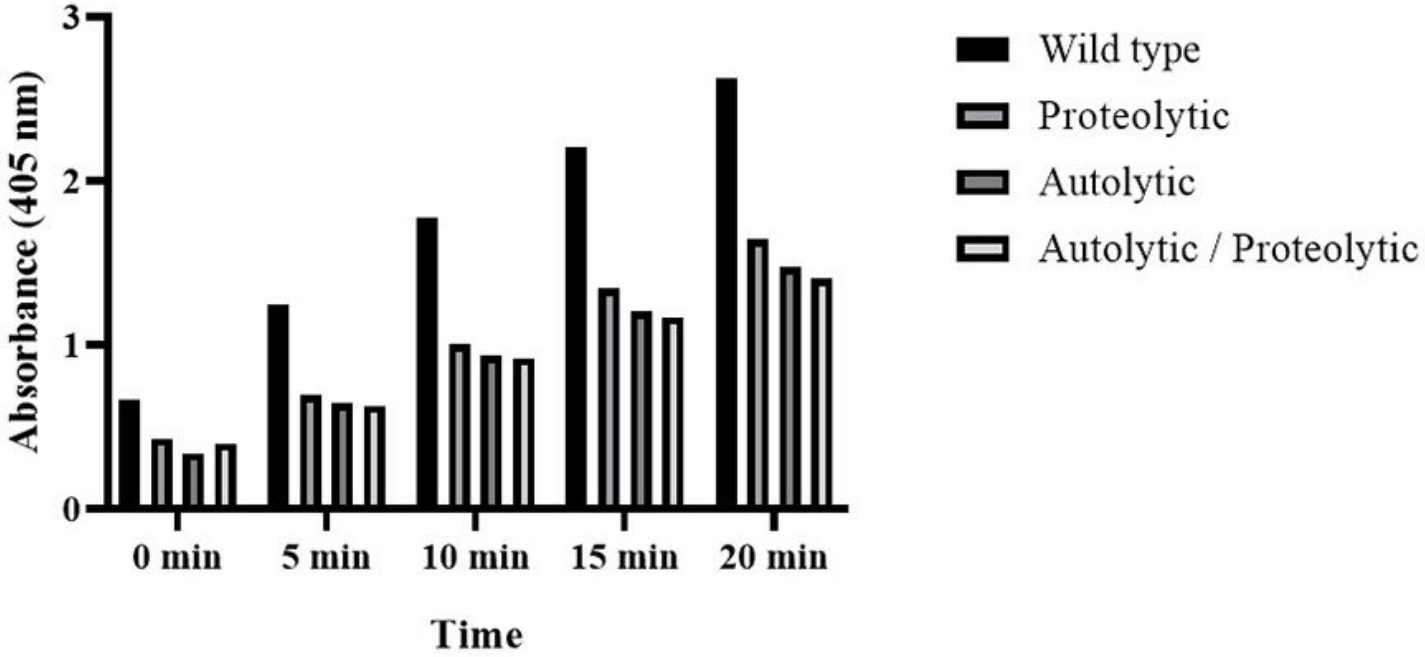

Figure 6

Hydrolytic activity assay of ocriplasmin variants measured at 405 nm. The product formation (color intensity) of mutant variants presented much rapid reduction, compared to the wild-type. Data indicate mean of duplicate measurements and analyzed by one-way ANOVA test for detecting significant differences compared to wild-type (P<0.01)

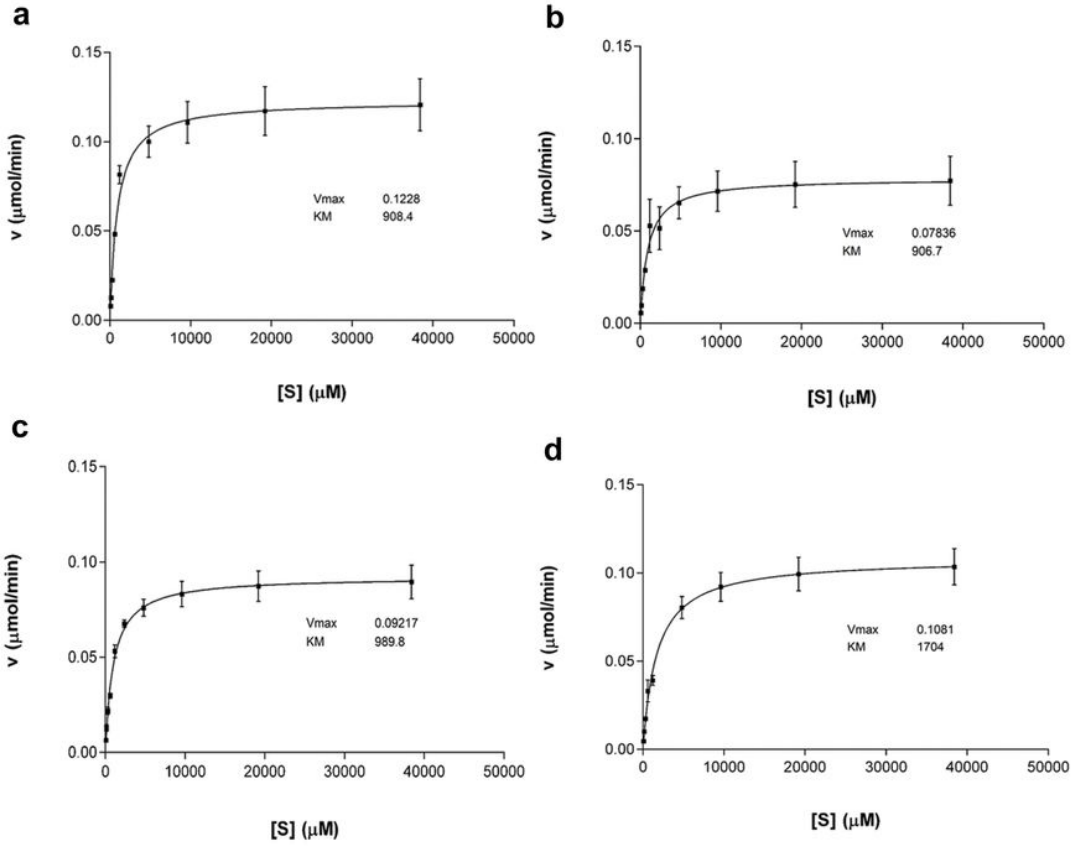

Figure 7

kinetic parameters of the wild-type and mutant variants of Ocriplasmin. a wild-type, b proteolytic, c autolytic and d mixed variants with the substrate S-2403 on the basis of the Michaelis–Menten plot at 37 °C